Inorg. Chem. **2005**, *44*, 1554−1562

Homo- and Heterobimetallic Niobium^{V} and Tantalum^{V} Peroxo-tartrate Complexes and Their Use as Molecular Precursors for Nb−Ta Mixed Oxides

Daisy Bayot,[†] Bernard Tinant,[‡] and Michel Devillers*,[†]

Unité de Chimie des Matériaux Inorganiques et Organiques, and Unité de Chimie Structurale et des Mécanismes Réactionnels, Université Catholique de Louvain, Place Louis Pasteur 1, B-1348 Louvain-la-Neuve, Belgium

Received November 9, 2004

New water-soluble bimetallic peroxo-tartrato complexes of niobium(V) and/or tantalum(V) have been prepared, characterized from the structural and spectroscopic point of view, and used as molecular precursors for Nb−Ta mixed oxides. Two new homometallic complexes, $(gu)_5[Nb_2(O_2)_4(tart)(Htart)]\cdot 4H_2O$ (**1a**) and $(gu)_6[Ta_2(O_2)_4(tart)_2]\cdot 4H_2O$ (**2a**), and the corresponding heterometallic complex, $(gu)_5[NbTa(O_2)_4(tart)(Htart)]\cdot 4H_2O$ (**3**), have been obtained. The crystal structures of the homometallic compounds, $(gu)_5[Nb_2(O_2)_4(tart)(Htart)]\cdot 6H_2O\cdot 1H_2O_2$ (**1b**) and $(gu)_6[Ta_2(O_2)_4(tart)_2]\cdot 6H_2O$ (**2b**), have been determined, showing, for both cases, two 8-fold-coordinated metal atoms, each surrounded by oxygen atoms belonging to two bidentate peroxides, two monodentate carboxylato, and two alkoxo groups from both bridging tartrato ligands. The coordination polyhedron around each metal atom is a dodecahedron. The thermal treatment of complexes **1a**, **2a**, and **3** in air at 700 or 800 °C, depending of the Ta content, provided Nb_2O_5, Ta_2O_5, and the solid solution $TaNbO_5$, respectively. The thermal treatment of a 1:1 Nb/Ta molar ratio mixture of **1a** and **2a** has also been studied. BET and SEM measurements have been carried out and reveal these oxides possess relatively high specific surface areas and display a porous character. Comparison between the use of homo- and heterometallic precursors is discussed.

I. Introduction

In past decades, multicomponent Nb-containing oxide materials have generated considerable interest in many fields, because of their attractive physical properties. Such oxides are, for example, widely studied as ferroelectric and piezoelectric materials such as $BiNbO_4$,[1] as ion conductors such as Y_3NbO_7,[2] and also promising catalysts in several highly challenging processes, like water photodecomposition,[3−7] alkane oxidation, or ammoxidation.[8,9] Within the same context, analogous Ta-based oxides, like $BiTaO_4$[5,7] and $TaVO_5$,[10] were also reported but in a very less extended way than for niobium. The literature describes mainly solid solutions between niobium and tantalum pentoxides[3,4,11,12] which are essentially studied in the context of water photodecomposition under UV irradiation.[3,4] In particular, associating niobium and tantalum pentoxide in a common lattice produces ordered mesoporous materials that could be used, according to the authors, in the domains of catalysis, sorption, sensing, as well as nano-devices.[13]

The conventional way to prepare oxide materials is based on solid-state reactions between the binary oxides. This so-

* Author to whom correspondence should be addressed. E-mail: devillers@chim.ucl.ac.be.
[†] Unité de Chimie des Matériaux Inorganiques et Organiques.
[‡] Unité de Chimie Structurale et des Mécanismes Réactionnels.

(1) Ayyub, P.; Multani, M. S.; Palmkar, V. R.; Vijayaraghavan, R. *Phys. Rev. B* **1986**, *34*, 8137−8140.
(2) Okubo, T.; Kakihana, M. *J. Alloys Compd.* **1997**, *256*, 151−154.
(3) Katou, T.; Lee, B.; Lu, D. L.; Kondo, J. N.; Hara, M.; Domen, K. *Angew. Chem., Int. Ed.* **2003**, *42*, 2382−2385.
(4) Kondo, J. N.; Yamashita, T.; Katou, T.; Lee, B.; Lu, D.; Hara, M.; Domen, K. *Stud. Surf. Sci. Catal.* **2002**, *141*, 265−272.
(5) Zou, Z. G.; Ye, J. H.; Arakawa, H. *Solid State Commun.* **2001**, *119*, 471−475.
(6) Zou, Z. G.; Ye, J. H.; Arakawa, H. *Chem. Mater.* **2001**, *13*, 1765−1769.
(7) Zou, Z. G.; Arakawa, H.; Ye, J. H. *J. Mater. Res.* **2002**, *17*, 1446−1454.
(8) Ushikubo, T. *Catal. Today* **2000**, *57*, 331−338.
(9) Watling, T. C.; Deo, G.; Seshan, K.; Wachs, I. E.; Lercher, J. A. *Catal. Today* **1996**, *28*, 139−145.
(10) Amarilla, J. M.; Casal, B.; Ruiz-Hitzky, E. *J. Mater. Chem.* **1996**, *6*, 1005−1011.
(11) Yamagushi, O.; Tomihisa, D.; Shirai, M.; Shimizu, K. *J. Am. Ceram. Soc.* **1988**, *71*, 260−262.
(12) Zafrir, M.; Aladjem, A.; Zilber, R. *J. Solid State Chem.* **1976**, *18*, 377−380.

10.1021/ic0484250 CCC: $30.25
Published on Web 02/04/2005

called "ceramic method" requires heat treatments at a relatively high temperature, classically beyond 1000 °C, as well as repeated grinding procedures. It generally results in samples of low purity, in which several ternary oxides of various stoichiometries may coexist also with residual reactants. Because of these limitations, alternative routes such as sol−gel synthesis, citrate method, metal−organic chemical vapor deposition (MOCVD), or pyrolytic decomposition are often considered. These methods, requiring metal−organic precursors which have specific chemical and physical properties, present some obvious advantages: (i) the use of molecular precursors provides homogeneous materials due to mixing of the metals at the molecular level; (ii) these "precursor routes" that allow crystalline oxides to form under conditions significantly milder than those employed in conventional solid-state synthesis[14,15] result in materials with relatively high specific surface areas; and (iii) the presence of bridging or chelating organic ligands in the precursors has been shown to avoid unwanted metal segregation during oxide formation.[16] More particularly, when different metals are involved in the final oxide formulation, the main advantage of such routes is the potential use of heterometallic single-source precursors, when available, which provide a much greater control of the metal stoichiometry in the final oxide.[17−19] Ideally, precursor complexes containing the number of metal atoms corresponding to the stoichiometry of the desired oxide phase are required to optimize the approach, but this often represents an ambitious challenge.

The Nb- or Ta-based heterometallic compounds described so far are exclusively alkoxide-type precursors, which, unfortunately, present several drawbacks such as their moisture sensitivity or expensiveness. The described heterometallic complexes of Nb or Ta with oxo and/or alkoxo ligands only are numerous. Compounds such as $Nb_2(OMe)_2(ReO_4)_2$, $M_2O_2(OMe)_{14}(ReO_4)_2$ (M = Nb or Ta),[20] $Mg[Nb(OEt)_6]_2 \cdot 2EtOH$, $Sr[Ta(OiPr)_6]_2 \cdot 2Pr^iOH$,[21] $Mo_4M_2O_8(O^iPr)_{14}$, and $Mo_4M_4O_{16}(O^iPr)_{12}$ (M = Nb or Ta)[22] have been reported recently. Next to that, the association of the metal alkoxides with ligands such as halides, acetate, carboxylates, or β-diketonates can be considered as a way to overcome the difficulty of handling them. Several acetato-alkoxo-based heterometallic compounds with Nb such as $MNb_2(OAc)(O^iPr)_{10}$ (M = Mg, Cd, or Pb)[16,23] have been studied as precursors for the corresponding MNb_2O_6 phase. Also, some acetylacetonate derivatives such as $M^{II}_2M^V_2(acac)_2(OMe)_{12}$ (M^{II} = Co, Ni, Zn, or Mg and M^V = Nb or Ta)[24] are known. Moreover, very recently, two heterometallic Nb- or Ta- and Bi-based compounds with salicylate ligands, $Bi_2M_2(\mu\text{-}O)(sal)_4(Hsal)_4(OEt)_2$ and $BiM_4(\mu\text{-}O)_4(sal)(Hsal)_3(O^iPr)_4$,[18,19] have been reported as single-source precursors for the ferroelectric $BiMO_4$ phase. Only two mixed niobium and tantalum heterometallic complexes have been described so far: the homoleptic alkoxide $NbTa(OMe)_{10}$[25] and the heteroleptic compound $[Ta(O^iPr)_4]Nb(tea)$ (tea = triethanolamine).[26]

Because of the growing importance of Nb- and Ta-based oxide materials and the lack of described Nb−Ta heterometallic complexes, research on niobium^V and tantalum^V coordination compounds that could be used as single-source molecular precursors for the preparation of Nb−Ta-based oxides is therefore welcome. We report here the synthesis and characterization of novel air-stable and water-soluble homo- and heterobimetallic complexes of Nb^V and Ta^V with peroxo and tartrato ligands. The formation of a solid solution between Nb_2O_5 and Ta_2O_5 from the thermal decomposition of the prepared complexes is also investigated.

II. Experimental Section

General. Tartaric acid, DL-H_4tart (ACROS), and hydrogen peroxide, H_2O_2 (35 wt %, Acros), were commercial products used as received. Elemental analyses (C, H, N) of the complexes were carried out at the University College of London. IR spectra in the 4000−400 cm^{-1} range were recorded on a FTS-135 Bio-RAD spectrometer, using KBr pellets containing ca. 1 wt % of the powder. Thermogravimetric analyses (TGA) were performed in air at the heating rate of 10 °C/min using a Mettler Toledo TGA/SDTA851^e analyzer. Nano-electrospray ionization mass spectrometry (NESI-MS) measurements were obtained on a Finnigan MAT LCQ instrument (San Jose, CA). The samples were introduced by injection of a 0.001 mol/L solution of the complex dissolved in CH_3OH/H_2O (1:1 vol). FT-Raman spectra were recorded on a Bruker spectrometer (type RFS100/S) at the wavelength of 1064 nm. Powder XRD was carried out on a SIEMENS D-5000 diffractometer using the Cu Kα radiation. BET specific surface areas were measured with a Micromeritics ASAP 2000 analyzer using nitrogen at 77 K. The SEM studies were carried out on a DSM982 GEMINI microscope operating at a 1 kV accelerating voltage. The EDX microanalyses were carried out with the same device on a Nb−Ta heteronuclear crystal and on a powder sample of a $NbTaO_5$ oxide as reference material. Both the observation of the samples and the analyses were measured with 15 kV accelerating voltage.

Syntheses of the Precursors. All of the manipulations were carried out in aqueous solution. The starting reactants, $(gu)_3[M(O_2)_4]$ (M = Nb or Ta), were previously synthesized, according to reported procedures,[27,28] from niobic or tantalic acid in the presence of an excess of H_2O_2 and guanidinium carbonate, $(gu)_2CO_3$ (Aldrich).

(13) Lee, B.; Yamashita, T.; Lu, D. L.; Kondo, J. N.; Domen, K. *Chem. Mater.* **2002**, *14*, 867−875.
(14) Camargo, E. R.; Kakihana, M. *Solid State Ionics* **2002**, *151*, 413−418.
(15) Wullens, H.; Leroy, D.; Devillers, M. *Int. J. Inorg. Mater.* **2001**, *3*, 309−321.
(16) Boulmaaz, S.; Papiernik, R.; Hubert-Pfalzgraf, L. G.; Septe, B.; Vaissermann, J. *J. Mater. Chem.* **1997**, *7*, 2053−2061.
(17) Hubert-Pfalzgraf, L. G. *Inorg. Chem. Commun.* **2003**, *6*, 102−120.
(18) Thurston, J. H.; Whitmire, K. H. *Inorg. Chem.* **2002**, *41*, 4194−4205.
(19) Thurston, J. H.; Whitmire, K. H. *Inorg. Chem.* **2003**, *42*, 2014−2023.
(20) Shcheglov, P. A.; Drobot, D. V.; Seisenbaeva, G. A.; Gohil, S.; Kessler, V. G. *Chem. Mater.* **2002**, *14*, 2378−2383.
(21) Jones, A. C.; Davies, H. O.; Leedham, T. J.; Wright, P. J.; Crosbie, M. J.; Steiner, A.; Bickley, J. F.; O'Brien, P.; White, A. J. P.; Williams, D. J. *J. Mater. Chem.* **2001**, *11*, 544−548.
(22) Johansson, A.; Roman, M.; Kessler, V. G. *J. Sol.-Gel Sci. Technol.* **2000**, *19*, 725−728.
(23) Hubert-Pfalzgraf, L. G. *Polyhedron* **1994**, *13*, 1181−1195.
(24) Werndrup, P.; Kessler, V. G. *J. Chem. Soc., Dalton Trans.* **2001**, *5*, 574−579.
(25) Hubert-Pfalzgraf, L. G.; Riess, J. G. *Inorg. Chem.* **1975**, *14*, 2854−2856.
(26) Sharma, M. K.; Singh, A.; Mehrotra, R. C. *Transition Met. Chem.* **2002**, *27*, 115−119.
(27) Bayot, D.; Tinant, B.; Devillers, M. *Catal. Today* **2003**, *78*, 439−447.
(28) Bayot, D.; Tinant, B.; Devillers, M. *Inorg. Chem.* **2004**, *43*, 5999−6005.

Niobic acid, $Nb_2O_5 \cdot nH_2O$, was supplied from CBMM (Brazil), and tantalic acid was prepared by hydrolysis of tantalum chloride, $TaCl_5$ (Alfa Aesar), in ammonia medium.

$(gu)_5[Nb_2(O_2)_4(tart)(Htart)] \cdot 4H_2O$ (1a). $(gu)_3[Nb(O_2)_4]$ (0.413 g, 1.03 mmol) and DL-H_4tart (0.152 g, 1.03 mmol) were dissolved in distilled water (10 mL) while stirring. The solution was treated with 5 mL of a 35 wt % H_2O_2 solution and then gently heated for a few minutes ($T = 70$ °C). Cooling the solution down to room temperature yielded small colorless crystals, which were filtered off (**1a**). Yield 0.58 g (54%). Anal. Calcd for $C_{13}H_{43}N_{15}Nb_2O_{24}$: C, 15.95; H, 4.29; N, 21.47. Found: C, 15.94; H, 4.08; N, 20.96.

The X-ray diffraction analysis was carried out on crystals kept in solution, within 1 h after their appearance because of fast decomposition. They correspond to the stoichiometry $(gu)_5[Nb_2(O_2)_4(tart)(Htart)] \cdot 6H_2O \cdot 1H_2O_2$ (**1b**).

$(gu)_6[Ta_2(O_2)_4(tart)_2] \cdot 4H_2O$ (2a). $(gu)_3[Ta(O_2)_4]$ (1.20 g, 2.46 mmol) and DL-H_4tart (0.368 g, 2.46 mmol) were dissolved in distilled water (20 mL) while stirring. The solution was treated with 5 mL of a 35 wt % H_2O_2 solution and then gently heated for a few minutes ($T = 70$ °C). Cooling slowly the solution down to room temperature yielded small colorless crystals, which were filtered off (**2a**). Yield 1.04 g (36%). Anal. Calcd for $C_{14}H_{48}N_{18}Ta_2O_{24}$: C, 13.84; H, 3.96; N, 20.76. Found: C, 13.79; H, 3.68; N, 20.03.

Some of the obtained crystals were kept in solution and analyzed by X-ray diffraction within 1 h after their appearance because of fast decomposition. They correspond to the stoichiometry $(gu)_6[Ta_2(O_2)_4(tart)_2] \cdot 6H_2O$ (**2b**).

$(gu)_5[NbTa(O_2)_4(tart)(Htart)] \cdot 4H_2O$ (3). $(gu)_3[Nb(O_2)_4]$ (0.501 g, 1.25 mmol), $(gu)_3[Ta(O_2)_4]$ (0.610 g, 1.25 mmol), and DL-H_4tart (0.374 g, 2.52 mmol) were dissolved in distilled water (20 mL) while stirring. The solution was treated with 5 mL of a 35 wt % H_2O_2 solution and then gently heated for a few minutes ($T = 70$ °C). Cooling slowly the solution down to room temperature yielded small colorless crystals, which were filtered off (**3**). Yield 0.81 g (62%). Anal. Calcd for $C_{13}H_{43}N_{15}NbTaO_{24}$: C, 14.62; H, 4.03; N, 19.68. Found: C, 14.55; H, 3.86; N, 20.53.

Some of the obtained crystals were kept in solution and analyzed by X-ray diffraction within 1 h after their appearance because of fast decomposition.

X-ray crystallography. The X-ray intensity data were collected at 110 K for **1b** and **2b** with a MAR345 image plate using Mo Kα ($\lambda = 0.71069$ Å) radiation. The selected crystal was mounted in inert oil and transferred to the cold gas stream for flash cooling. The crystal data and data collection parameters are summarized in Table 1. The unit cell parameters were refined using all of the collected spots after the integration process. The data were not corrected for absorption, but the data collection mode partially takes the absorption phenomena into account (100 images, $\Delta\Phi = 3°$, 24 145 reflections measured for 3879 independent for **1b**; 200 images, $\Delta\Phi = 3°$, 43 023 reflections measured for 3893 independent for **2b**). The structure of complex **1b** was solved by direct methods with SHELXS97.[29] The structure of **2b** is isomorphous with that of **1b**. Both structures were refined by full-matrix least-squares on F^2 using SHELXL97.[29] All of the non-hydrogen atoms were refined with anisotropic temperature factors except the oxygen atoms of two water molecules of **2b** (O200 and O300) and O400 of the hydrogen peroxide molecule in **1b**, which were refined isotropically because of high thermal agitation. The hydrogen atoms were calculated with AFIX and included in the refinement with a common isotropic temperature factor. The H atoms of one of the three water molecules in structure **1b** (O100) could be localized by Fourier-difference synthesis, but all of the other hydrogen of water or peroxides molecules were not localized. The details of the refinement and the final R indices are presented in Table 1. In each structure, the largest peak in the final Fourier difference synthesis is located near the heavy atom.

Table 1. Crystallographic Data and Structure Refinement Parameters for **1b** and **2b**

	1b	2b
formula	$C_{13}H_{49}N_{15}Nb_2O_{28}$	$C_{14}H_{52}N_{18}Ta_2O_{26}$
fw	1049.5	1250.6
T (K)	110(2)	110(2)
crystal system	monoclinic	monoclinic
space group	$C2/c$	$C2/c$
unit cell dimensions		
a (Å)	19.747(7)	19.962(7)
b (Å)	15.608(5)	15.533(5)
c (Å)	12.295(4)	12.261(4)
α (deg)	90	90
β (deg)	90.81(2)	90.76(2)
γ (deg)	90	90
Z	4	4
V (Å^3)	3789(2)	3801(2)
D_{calcd} (g cm^{-3})	1.84	2.18
μ (mm^{-1})	0.72	5.83
F (000)	2140	2412
crystal size (mm)	0.40 × 0.30 × 0.18	0.24 × 0.24 × 0.16
θ range (deg)	3.09−26.73	2.62−26.39
hkl ranges	$0 \le h \le 24$	$0 \le h \le 24$
	$0 \le k \le 19$	$0 \le k \le 19$
	$-15 \le l \le 15$	$-15 \le l \le 15$
reflns collected/unique	24 145/3879	43 023/3893
R_{int}	0.032	0.065
data/restraints/parameters	3879/6/266	3893/29/265
R_1, wR_2 [$I > 2\sigma(I)$][a]	0.057, 0.154 [3259]	0.057, 0.125 [3667]
R_1, wR_2 (all data)	0.057, 0.154	0.059, 0.126
GOF on F^2	1.19	1.15
largest diff. peak (e Å^{-3})	1.92/−1.22	2.64/−3.13

[a] $R1 = \sum||F_o| - |F_c||/\sum|F_o|$, $wR2 = [(|F_o^2 - F_c^2)^2/\sum(wF_o^2)^2]^{1/2}$.

Pyrolysis of the Precursors. A sample (approximately 0.5 g) of each obtained complex (**1a**, **2a**, and **3**) as well as a ground mixture of **1a** and **2a** (Nb/Ta molar ratio = 1) were placed in a porcelain dish and precalcined at 300 °C for 6 h in air, yielding an amorphous material which was then calcined for 6 h in air, at 700 °C or 800 °C, depending on the Ta content.

Synthesis of the $TaNbO_5$ EDX Reference Phase. The $TaNbO_5$ oxide was prepared by a reported chelate method[30] using water-soluble niobium and tantalum coordination compounds, $(gu)_3[Nb(O_2)_2(edtaO_2)] \cdot 2H_2O$ and $(gu)_3[Ta(O_2)_2(edtaO_2)] \cdot 2H_2O$, as metal precursors. Both compounds were dissolved together and simultaneously in distilled water according to the appropriate proportion (Nb/Ta = 1). The resulting clear solution was then stirred at room temperature during 1 h. The solvent was gently eliminated by a freeze-drying process, and the Nb−Ta mixed solid precursor obtained was then precalcined at 300 °C for 6 h in air, yielding an amorphous material which was then calcined at 700 °C for 6 h in air. The formation of the $TaNbO_5$ phase was evidenced by Raman spectroscopy and powder X-ray diffraction.

III. Results and Discussion

III. 1. Complexes. General Comments. The presence of peroxo ligands in the niobium and/or tantalum complexes enhances their solubility in water. These compounds constitute therefore ideal candidates as precursors for the

(29) Sheldrick, G. M. *Program for crystal structure refinement*; University of Göttingen, Germany, 1997.

(30) Bayot, D.; Devillers, M. *Chem. Mater.* **2004**, *16*, 5401−5407.

Table 2. Infrared Data (in cm^{-1}) for Compounds **1a**, **2a**, and **3**[a]

	ν_{as}(COO)	ν_s(COO)	ν(O−O)	ν_{as}[M(O_2)]	ν_s(O−M−O)
1a	1654 sb	1363 m	850 m, 866 m	571 m	536 m
2a	1655 sb	1383 m	840 m, 847 m	581 m	539 w
3	1654 sb	1374 m	840 m, 850 mb, 840 m	570 m, 582 m	536 w, 541 w

[a] s = strong, m = medium, w = weak, b = broad.

Table 3. Data Deduced from TG Analyses for Compounds **1a**, **2a**, **3**, and a 1/1 Mixture of **1a** and **2a**

compound	T_F (°C)[a]	H_2O exp. (%)[b]	H_2O calc. (%)[c]
1a	600	6.63	6.93 ($n = 4$)
2a	730	5.21	5.93 ($n = 4$)
3	680	6.73	6.75 ($n = 4$)

[a] Final decomposition temperature. [b] Weight loss of the first decomposition step observed on the TG. [c] Calculated on the basis of the molecular formula containing n water molecule(s).

preparation of oxide materials and, more particularly, multimetallic oxides involving transition metals for which the availability of well-defined water-soluble complexes is very limited. Moreover, the use of nonmetallic guanidinium cations as counterions and of the tartrato ligand was particularly welcome to avoid residual contamination of the final materials upon thermal degradation under appropriate conditions. The guanidinium counterions also favor the stabilization of the crystal network by extensive H bonding.

IR Spectroscopy. Table 2 lists, for compounds **1a**, **2a**, and **3**, the infrared bands which are assigned to typical stretching vibration modes of the metal M coordinated side-bonded peroxo ligands ν(O−O), ν_{as}[M(O_2)], and ν_s(O−M−O), as well as some representative vibrational modes of the coordinated tartrato ligands. The IR spectra of the homometallic complexes **1a** and **2a** display two ν(O−O) bands of medium intensity at 850 and 866 cm^{-1} for the Nb derivative and at slighter values, 840 and 847 cm^{-1}, for the tantalum one. This spectral shape can be assigned to a metal-diperoxo species.[27,31] Moreover, the IR spectrum of the heterometallic complex **3** shows three ν(O−O) bands resulting from the superposition of the bands appearing in the spectra of the homometallic complexes. Next to this is the antisymmetric stretching frequency of the coordinated carboxylato groups, for the three compounds synthesized, as a strong broad band near 1650 cm^{-1}. Coordination of the metal atom by these carboxylato groups is evidenced by the broadening of this ν_{as}(COO) band and by its significant shift from a value of 1743 cm^{-1} in the free tartaric acid to ca. 1650 cm^{-1} in the complexes.

Thermal Analyses. After dehydration, the complexes **1a**, **2a**, and **3** undergo a multistep degradation into oxides up to a final decomposition temperature in the range 600−730 °C. Table 3 lists the final decomposition temperature as well as the number of crystallized water molecules deduced from the TG analyses. The thermograms of the three peroxo-tartrato compounds (**1a**, **2a**, and **3**) are illustrated in Figure 1a. Each analysis displays a slight weight loss (approximately 3%) corresponding to the last decomposition step that is characteristic of Nb and Ta compounds. In the case of the homometallic derivatives, this final step appears at 600 °C for the niobium complex **1a** and at 730 °C for the tantalum one **2a**. In the thermogram of a 1:1 molar ratio mixture of **1a** and **2a** (Figure 1b), two distinct steps appear at 600 and 730 °C, in line with the presence of the Nb and Ta homonuclear derivatives, respectively. In the thermogram of compound **3**, one single step occurs at the intermediate temperature of 680 °C, evidencing the heterometallic nature of this compound.

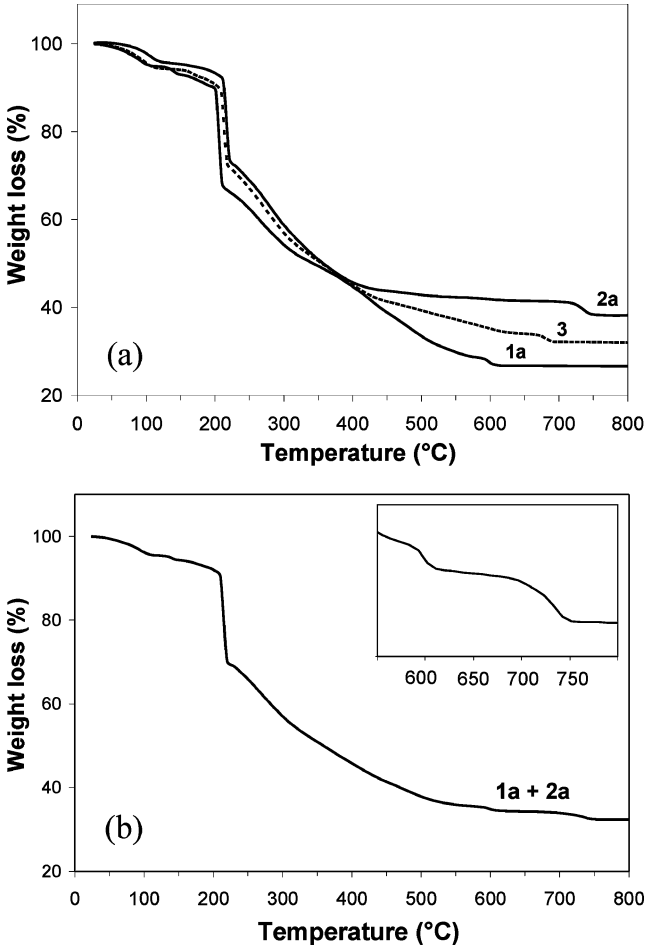

Figure 1. Thermogravimetric analyses in air (a) of **1a**, **2a**, **3**, and (b) of a 1:1 molar ratio mixture of **1a** and **2a** (10 °C/min).

Mass Spectrometry. Figure 2 displays the negative ion mass spectra obtained for compounds **1a**, **2a**, **3**, and for a 1:1 molar ratio mixture of **1a** and **2a**. The spectrum of compound **1a** shows major peaks at m/z 601.7 and 694.5, assignable to the singly charged species $(gu[Nb_2(O_2)_2(tart)(tart)])^-$ and $((gu)_2[Nb_2(O_2)_3(tart)(Htart)])^-$, respectively. The first fragment corresponds to the parent ion that has lost two peroxo groups and one H^+ from the protonated tartrato ligand, and is combined with one guanidinium counterion. The second fragment corresponds to the parent ion that has lost one peroxo group and is combined with two gu^+. Next to that, species corresponding to the loss of the $tart^{4-}$ or $Htart^{3-}$ ligand, $(gu[Nb_2(O_2)_4(Htart)])^-$ and $(gu[Nb_2(O_2)_4(tart)])^-$, are also observed at m/z 460.6 and 519.5, respectively. The most intense peaks observed in the

(31) Bayot, D.; Tinant, B.; Mathieu, B.; Declercq, J. P.; Devillers, M. *Eur. J. Inorg. Chem.* **2003**, 737−743.

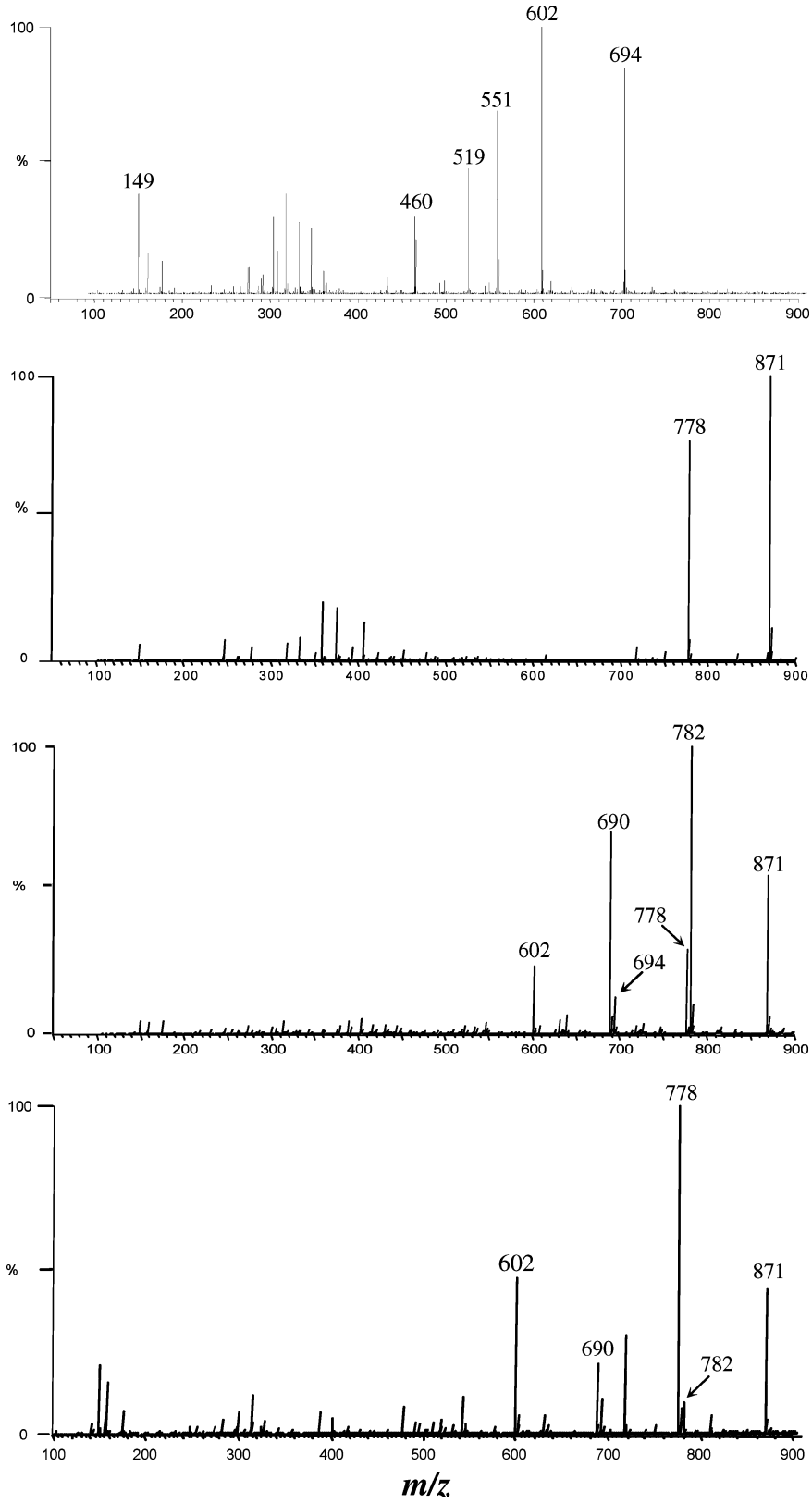

Figure 2. NESI-mass spectrum (anionic mode) of (a) **1a**, (b) **2a**, (c) **3**, and (d) a 1:1 molar ratio mixture of **1a** and **2a** in a 1:1 vol methanol−water medium.

mass spectrum of the tantalum complex **2a** (m/z = 777.7 and 870.6) correspond to fragments similar to those obtained for the Nb derivative, $(gu[Ta_2(O_2)_2(tart)_2])^-$ and $(H(gu)_2[Ta_2(O_2)_3(tart)_2])^-$, respectively. The mass spectrum of the heterometallic compound **3** shows two intense peaks at m/z 689.6 and 782.5 that correspond to the singly charged ions $(gu[NbTa(O_2)_2(tart)_2])^-$ and $((gu)_2[NbTa(O_2)_3(tart)(Htart)])^-$, respectively.

Next to that, peaks corresponding to both homometallic complexes **1a** (m/z 601.7 and 694.5) (m/z 777.7 and 870.5)

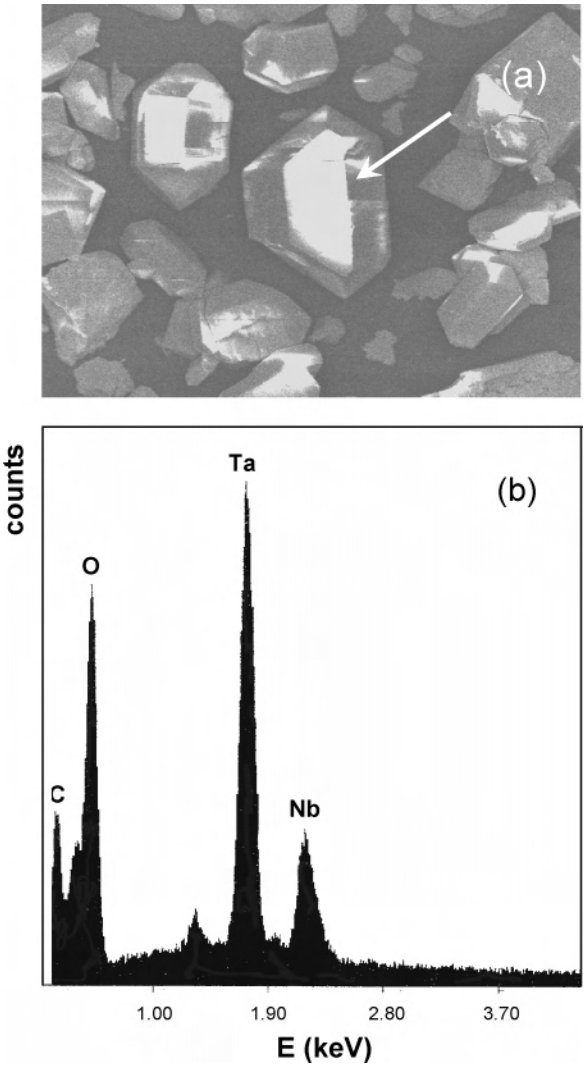

Figure 3. (a) SEM image and (b) EDX spectrum of a monocrystal of **3**. The analysis was performed at the point indicated by the arrow.

Table 4. Selected Bond Lengths (Å) for **1b** and **2b** (M = Nb or Ta)

	1b	2b
	Carboxylate	
M−O5	2.134(2)	2.126(6)
M−O9	2.135(2)	2.128(6)
	Alkoxo/Hydroxo	
M−O7	2.181(3)	2.071(6)
M−O8	2.014(3)	2.034(6)
	Peroxo	
M−O1	2.002(3)	2.024(6)
M−O2	1.992(3)	2.010(6)
M−O3	2.000(3)	2.015(7)
M−O4	1.997(4)	2.029(7)
O1−O2	1.493(2)	1.518(9)
O3−O4	1.500(2)	1.507(8)

and **2a** are present in the spectrum of **3**. This observation indicates either the occurrence of dissociation-recombination phenomena during the spray formation or in gaseous phase, or the presence of undesirable homometallic species in the analyzed solution that would come from the sample itself or from a dissociation-recombination process in solution that generates the homometallic complexes from the heterometallic one.

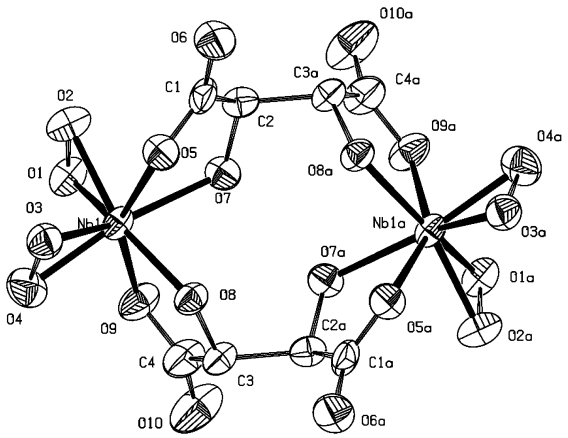

Figure 4. ORTEP plot of the molecular anion of **1b**, $[Nb_2(O_2)_4(tart)(Htart)]^{5-}$ (50% probability).

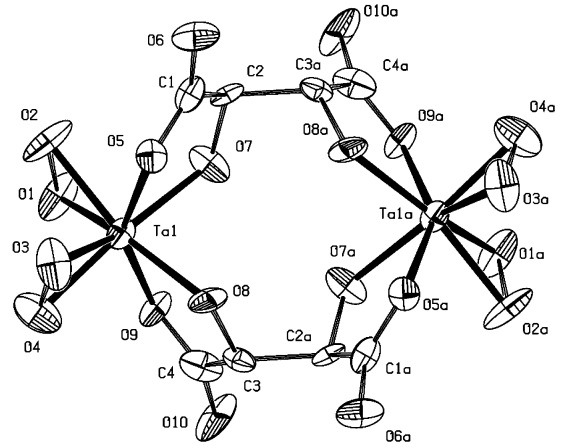

Figure 5. ORTEP plot of the molecular anion of **2b**, $[Ta_2(O_2)_4(tart)_2]^{6-}$ (50% probability).

To elucidate that point, we measured the response of a 1:1 molar ratio mixture of both homometallic species **1a** and **2a** and observed that the mass spectrum obtained (Figure 2d) evidences the formation of small amounts of the heterometallic complex (peaks of relatively low intensity at *m*/*z* 690.0 and 782.7) from the two homometallic compounds. Moreover, no dissociation-recombination phenomenon in solution was observed as proven by the following experiment: a 1:1 molar ratio mixture of **1a** and **2a** was stirred in aqueous medium during 1 h at room temperature, and then the solution was cooled and the resulting crystalline product was isolated and analyzed by thermogravimetry. The obtained thermogram displayed the characteristic slight weight loss of each Nb and Ta homometallic compound, at 600 and 730 °C, respectively, but no step at 680 °C that could evidence the presence of the heterometallic species. The peaks assignable to the homonuclear complexes observed in the mass spectrum of **3** come from a dissociation-recombination process occurring during the analysis.

SEM/EDX. SEM/EDX analyses were performed on numerous monocrystals of **3**, and representative results are displayed in Figure 3. This EDX spectrum presents peaks characteristic of niobium and tantalum, at 2.166 (Kα) and 1.710 (Mα) keV, respectively. The area ratio of the Ta/Nb peaks is equal to 3.03 in comparison with the value of 3.07

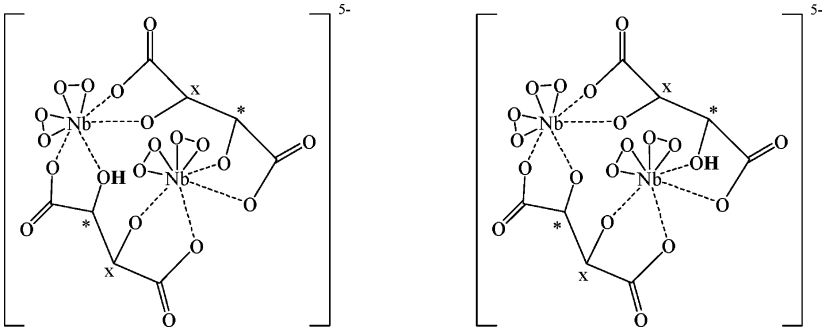

Figure 6. Schematic representation of the sharing of an acidic proton between two crystallographic equivalent sites in the tartrato ligand.

obtained for the $TaNbO_5$ reference material in which the Ta/Nb molar ratio is known to be equal to 1. This result strengthens the idea that compound **3** is a heteronuclear species with a Ta/Nb molar ratio of 1.

X-ray Crystal Structures. The complexes **1b** and **2b** are isomorphous. Table 4 presents selected bond lengths for crystals **1b** and **2b**, and Figures 4 and 5 display the molecular structure of the $[Nb_2(O_2)_4(tart)(Htart)]^{5-}$ and $[Ta_2(O_2)_4(tart)_2]^{6-}$ anions, respectively. In these compounds, both tartrates are tetradentate and act as bridging ligands between the metal atoms. In both cases, the coordination is completed by two bidentate peroxo groups per metal atoms. Niobium and tantalum exhibit an 8-fold coordination by oxygen atoms belonging to two bidentate peroxides, two monodentate carboxylato, and two alkoxo groups from both bridging tartrato ligands. The coordination polyhedron observed in both cases is a dodecahedron, as already observed in all Nb or Ta peroxo compounds described so far in the literature.[27,28,31−37] In crystal **1b**, the coordination distances are in the range of the values already reported for Nb peroxo complexes.[27,31−36] The Nb−O(carboxylato) distances are 2.134(3) and 2.135(3) Å, while the Nb−O(alkoxo) bond distances reach 2.014(3) and 2.181(3) Å. The Nb−O(peroxo) bond lengths range from 1.992(3) to 2.002(3) Å with a mean value of 1.997(3) Å, and the (O−O) distances reach 1.493(4) and 1.500(4) Å. In crystal **2b**, the values for Ta−O(carboxylato) bonds are 2.126(6) and 2.128(6) Å, and the Ta−O(alkoxo) bond distances reach 2.034(6) and 2.071(6) Å. The Ta−O(peroxo) bond lengths range from 2.010(6) to 2.029(7) Å with a mean value of 2.019 Å, and the (O−O) distances are 1.518(9) and 1.507(8) Å. The metal−oxygen bond distances obtained for the Nb derivative are not significantly different from those of the Ta complex. This is in good agreement with the empirical rule from Brown et al. providing a cation−oxygen bond distance for a given valence: the Nb^V−O and Ta^V−O bond lengths obtained by theoretical calculations are identical.[38] The main difference between both compounds is the number of guanidinium cations: six for the tantalum derivative while five for the niobium one, which implies in that case the presence of an additional acidic proton carried by a tartrato ligand. While the two Nb−O(alkoxo) bond lengths in **1b** are significantly different from each other (Nb1−O8 = 2.014(3) Å and Nb1−O7 = 2.181(3) Å), it is not the case for the Ta−O(hydroxo) in **2b**; consequently, the additional proton in **1b** is probably localized on the O7 oxygen atom belonging to a tartrato ligand. However, this implies the molecular anion to be noncentrosymmetric, which is in

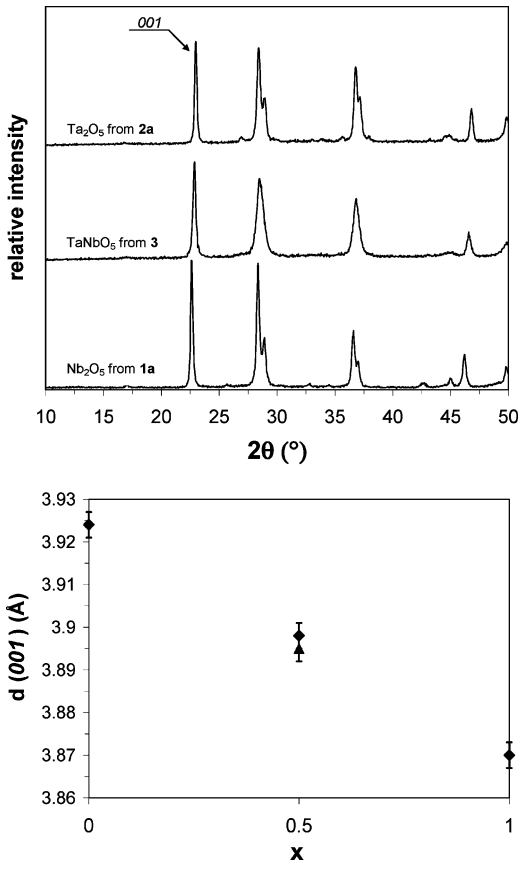

Figure 7. (a) X-ray diffraction patterns of the $(Ta_xNb_{1-x})_2O_5$ oxides obtained from **1a**, **2a**, and **3** ($x = 0$, 1, 0.5, respectively) and (b) evolution of the interreticular distance $d(001)$ versus the amount of tantalum, x (the triangle corresponds to the value obtained from a 1:1 molar mixture of **1a** and **2a**).

(32) de Oliveira, V.; San Gil, R. A. D.; Lachter, E. R. *Polyhedron* **2001**, *20*, 2647−2649.
(33) Mathern, G.; Weiss, R. *Acta Crystallogr., Sect. B* **1971**, *27*, 1598−1609.
(34) Mathern, G.; Weiss, R. *Acta Crystallogr., Sect. B* **1971**, *27*, 1572−1581.
(35) Mathern, G.; Weiss, R. *Acta Crystallogr., Sect. B* **1971**, *27*, 1582−1597.
(36) Passoni, L. C.; Siddiqui, M. R. H.; Steiner, A.; Kozhevnikov, I. V. *J. Mol. Catal. A* **2000**, *153*, 103−108.
(37) Wehrum, G.; Hoppe, R. *Z. Anorg. Allg. Chem.* **1993**, *619*, 1315−1320.
(38) Brown, I. D.; Wu, K. K. *Acta Crystallogr., Sect. B* **1972**, *32*, 1957−1959.

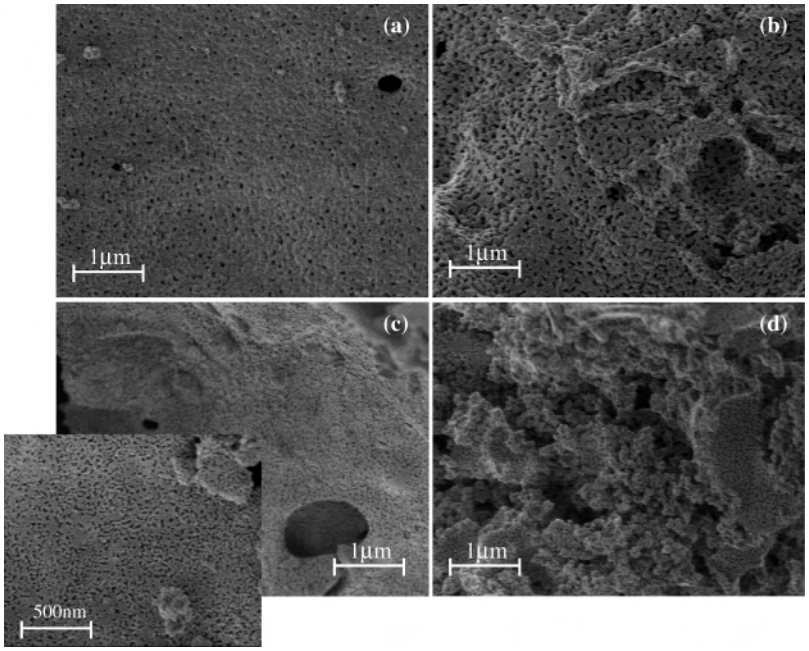

Figure 8. SEM images of the oxides obtained from (a) **1a**, (b) **2a**, (c) **3**, and (d) a 1:1 molar ratio mixture of **1a** and **2a**.

contradiction with the structural determination. To fulfill the symmetry requirements of the molecule, the site occupation factors of this proton on O7 and on its crystallographically equivalent site, O7a, must be both equal to 0.5. The proton is thus equally shared, as illustrated in Figure 6, between these two sites inside the crystalline network.

Three water molecules are cocrystallized in both structures. In complex **1b**, one additional hydrogen peroxide molecule is also observed. All of these solvent species are hydrogen bonded with the guanidinium cations, the oxygen atoms of the tartrato ligand, and between themselves.

X-ray diffraction was also performed on monocrystals of compound **3**. Preliminary measurements provided the symmetry and space group of the unit cell as well as the lattice parameters. This compound is isomorphous to **1b** and **2b**: monoclinic $C2/c$ with $a = 19.909(7)$ Å, $b = 15.540(5)$ Å, $c = 12.249(4)$ Å, and $\beta = 90.34(2)°$. No significant difference is observed for the heterometallic compound in comparison with the experimental parameters obtained for the homometallic Nb or Ta complexes.

III. 2. Oxides. X-ray Diffraction. The X-ray diffraction studies of the calcined Nb−Ta complexes show that the considered thermal treatment applied to the precursors leads to crystalline materials for all compositions. Figure 7a allows one to compare the XRD pattern of the oxide obtained from the heterometallic complex **3** to those of the corresponding binary oxides, Nb_2O_5 and Ta_2O_5, obtained from the homometallic compounds **1a** and **2a**, respectively. The similarity of the diffractograms suggests that the material prepared from **3** is isostructural with orthorhombic Nb_2O_5 (JCPDS file 30-0873) or Ta_2O_5 (JCPDS file 25-0922). However, slight shifts in 2θ values are actually observed for several diffraction peaks. The linear evolution of the interplanar distance $d(001)$ with the composition is illustrated in Figure 7b. The interplanar distance increases regularly with the tantalum content, x. A similar trend of the lattice evolution has been previously observed[11,13,30] but cannot be rationalized on the basis of the respective ionic radii of Nb^{5+} and Ta^{5+}, which are identical (0.74 Å).[39] This behavior evidences the formation of the ternary oxide $TaNbO_5$, corresponding to the $(Ta_xNb_{1-x})_2O_5$ solid solution with $x = 0.5$, by calcining the heterometallic complex **3**. Next to that, the pyrolysis of a 1:1 molar ratio mixture of **1a** and **2a** gives the same XRD results as for **3**.

Raman Spectroscopy. The Raman analyses confirmed these observations because the Raman spectra of the Nb and/or Ta oxides are all similar and exhibit a linear variation of the Raman shifts of several bands with the composition. When the Ta content increases, the intensity of these bands decreases and they are shifted to lower wavenumbers, in line with the fact that Ta is heavier than Nb. A similar behavior was previously observed for the $(Ta_xNb_{1-x})_2O_5$ solid solution.[30]

BET and SEM. BET and SEM measurements have been carried out to study the morphology of the oxides produced from the thermal decomposition of the prepared complexes. While the specific surface areas of the oxides obtained from **1a**, **2a**, and the 1:1 mixture of **1a** and **2a** are 14, 12, and 14 m^2/g, respectively, the material obtained from **3** displays a larger value of 30 m^2/g. These results indicate that the use of the heterometallic precursor **3** allows the preparation of mixed oxides with higher specific surface area.

SEM pictures of the oxides obtained are illustrated in Figure 8 and reveal the presence of macropores and mesopores. No morphology difference was observed between the oxides obtained from **3** and the one obtained from the mixture of **1a** and **2a** except that the pores are significantly smaller in the first case (estimated pore size 20−40 nm), in

(39) Shannon, R. D. *Acta Crystallogr., Sect. A* **1976**, *32*, 751−767.

line with the fact that this oxide possesses a higher specific surface area than the second one, derived from the mixture.

IV. Conclusion

New homo- and heterobimetallic niobium(V) and tantalum(V) complexes with peroxo ligands and tartaric acid have been prepared and characterized from the structural and spectroscopic point of view. The thermal decomposition in air of the prepared compounds was shown to provide binary (Nb_2O_5 or Ta_2O_5) or ternary ($TaNbO_5$) oxides with interesting morphology and surface characteristics. The mixed phase, obtained from the heterometallic Nb−Ta complex calcined at 700 °C, displays a porous character with an estimated pore size of 20−40 nm and a specific surface area of 30 m^2/g. The use of a heterometallic Nb−Ta complex as a "single-source precursor" presents several advantages from the point of view of preparation and material properties. Because of their high solubility in water, these compounds constitute ideal candidates as molecular precursors for Nb- and/or Ta-based materials (bulk or supported oxides, films, and coatings).

Acknowledgment. We thank the Belgian National Fund for Scientific Research (FNRS) for the research fellowship allotted to D.B. and financial support. We also thank CBMM Co. (Brazil) and Niobium Products Co. GmbH (Germany) for supplying niobic acid and for their financial support, and Prof. R. Legras for access to the SEM/EDX equipment.

Supporting Information Available: X-ray crystallographic file in CIF format for **1b** and **2b**. This material is available free of charge via the Internet at http://pubs.acs.org.

IC0484250